

## Complex Adsorption of Short Linear Alkanes in the Flexible Metal-Organic-Framework MIL-53(Fe)

P. L. Llewellyn,<sup>\*,†</sup> P. Horcajada,<sup>‡</sup> G. Maurin,<sup>§</sup> T. Devic,<sup>‡</sup> N. Rosenbach,<sup>§</sup> S. Bourrelly,<sup>†</sup> C. Serre,<sup>‡</sup> D. Vincent,<sup>†</sup> S. Loera-Serna,<sup>†</sup> Y. Filinchuk,<sup>||</sup> and G. Férey<sup>‡</sup>

Laboratoire Chimie Provence, Universités Aix-Marseille I, II et III - CNRS, UMR 6264, Centre de Saint Jérôme, 13397 Marseille, France, Institut Lavoisier (UMR CNRS 8180), Université de Versailles Saint-Quentin-en-Yvelines, 45 avenue des Etats-Unis, 78035 Versailles cedex, France, Institut Charles Gerhardt Montpellier, UMR CNRS 5253, UM2, ENSCM, UM1, Place E. Bataillon, 34095 Montpellier cedex 05 France, and SNBL at ESRF, 38043 Grenoble, France

Received April 6, 2009; E-mail: philip.llewellyn@univ-provence.fr

**Abstract:** This investigation is based on a combination of experimental tools completed by a computational approach to deeply characterize the unusual adsorption behavior of the flexible MIL-53(Fe) in the presence of short linear alkanes. In contrast to the aluminum or chromium analogues we previously reported, the iron MIL-53 solid, which initially exhibits a closed structure in the dry state, shows more complex adsorption isotherms with multisteps occurring at pressures that depend on the nature of the alkane. This behavior has been attributed to the existence of four discrete pore openings during the whole adsorption process. Molecular simulations coupled with *in situ* X-ray powder diffraction were able to uncover these various structural states.

### Introduction

Porous metal organic framework materials (MOFs) have found increasing interest since the past few years in potential applications such as separation and storage.<sup>1–3</sup> Encouraging results have been obtained recently in terms of hydrogen storage,<sup>4–6</sup> adsorption of green house gases,<sup>7–11</sup> liquid phase separation,<sup>12</sup> and drug delivery.<sup>13</sup> These solids may also present

additional properties in a number of domains including magnetism and luminescence, which arise from the possibility to change either their metal center or the organic linker. An exceptional property of some MOFs relies on their ability to adapt their pore opening to accommodate guest species, and different modes of flexibility have been described.<sup>14,15</sup> This effect, also called “breathing”, can produce a dramatic increase or decrease in cell volume without a loss of crystallinity or bond breaking.<sup>16</sup> Typical examples are the porous chromium or aluminum terephthalates denoted MIL-53 (M = Cr, Al)<sup>17,18</sup> (MIL stands for Materials from Institut Lavoisier) or M<sup>III</sup>(OH)•[O<sub>2</sub>C–C<sub>6</sub>H<sub>4</sub>–CO<sub>2</sub>]•x(solv), which are built up from chains of M(III) octahedra linked via terephthalate linkers to form a three-dimensional ordered structure with a one-dimensional channel system along the *c* axis. They exhibit either a *narrow pore* (np) monoclinic form (MIL-53(Cr,Al)np) or a *large pore* (lp) orthorhombic structure (MIL-53(Cr,Al)lp) depending on the amount of water or carbon dioxide adsorbed into the channels, leading to variations in cell volume up to 35% (Figure 1).<sup>17,18</sup> Adsorption of apolar molecules such as linear alkanes (C<sub>2</sub>–C<sub>9</sub>) gives rise to similar phenomena.<sup>19,20</sup>

<sup>†</sup> Universités Aix-Marseille I, II et III - CNRS.

<sup>‡</sup> Université de Versailles Saint-Quentin-en-Yvelines.

<sup>§</sup> Institut Charles Gerhardt Montpellier.

<sup>||</sup> SNBL at ESRF.

- (1) Férey, G. *Chem. Soc. Rev.* **2008**, *37* (1), 191–214.
- (2) Maji, T. K.; Kitagawa, S. *Pure Appl. Chem.* **2007**, *79* (12), 2155–2177.
- (3) Rowsell, J. L. C.; Yaghi, O. M. *Micr. Mes. Mat.* **2004**, *73* (1–2), 3–14.
- (4) Latroche, M.; Surlblé, S.; Serre, C.; Mellot-Draznieks, C.; Llewellyn, P. L.; Lee, J.-H.; Chang, J.-S.; Jhun, S. H.; Férey, G. *Angew. Chem., Int. Ed.* **2006**, *45*, 8227–8231.
- (5) Liu, Y.; Eubank, J. F.; Cairns, A. J.; Eckert, J.; Kravtsov, V. C.; Luebke, R.; Eddaoudi, M. *Angew. Chem., Int. Ed.* **2007**, *46*, 3278–3283.
- (6) Li, Y.; Yang, R. T. *Langmuir* **2007**, *23*, 12937–12944.
- (7) Bourrelly, S.; Llewellyn, P. L.; Serre, C.; Millange, F.; Loiseau, T.; Férey, G. *J. Am. Chem. Soc.* **2005**, *127*, 13519–13521.
- (8) Furukawa, H.; Miller, M. A.; Yaghi, O. M. *J. Mater. Chem.* **2007**, *17*, 3197–3204.
- (9) Llewellyn, P. L.; Bourrelly, S.; Serre, C.; Vimont, A.; Daturi, M.; Hamon, L.; De Weireld, G.; Chang, J.-S.; Hong, D.-Y.; Hwang, Y. K.; Jhung, S. H.; Férey, G. *Langmuir* **2008**, *24* (14), 7245–7250.
- (10) Llewellyn, P. L.; Bourrelly, S.; Serre, C.; Filinchuk, Y.; Férey, G. *Angew. Chem., Int. Ed.* **2006**, *45*, 7751–7754.
- (11) Serre, C.; Bourrelly, S.; Vimont, A.; Ramsahye, N. A.; Maurin, G.; Llewellyn, P. L.; Daturi, M.; Filinchuk, Y.; Leynaud, O.; Barnes, P.; Férey, G. *Adv. Mater.* **2007**, *19*, 2246–2251.
- (12) Alaerts, L.; Kirshhock, C. E. A.; Maes, M.; van der Veen, M. A.; Finsky, V.; Depla, A.; Martens, J. A.; Baron, G. V.; Jacobs, P. A.; Denayer, J. F. M.; De Vos, D. E. *Angew. Chem., Int. Ed.* **2007**, *46*, 4293–4297.

(13) Horcajada, P.; Serre, C.; Maurin, G.; Ramsahye, N. A.; Balas, F.; Vallet-Regi, M.; Sebban, M.; Taulelle, F.; Férey, G. *J. Am. Chem. Soc.* **2008**, *130*, 6774–6780.

(14) Li, D.; Kaneko, K. *Chem. Phys. Lett.* **2001**, *335*, 50–56.

(15) Kitaura, R.; Seki, K.; Akiyama, G.; Kitagawa, S. *Angew. Chem., Int. Ed.* **2003**, *42*, 428–431.

(16) Serre, C.; Mellot-Draznieks, C.; Surlblé, S.; Audebrand, N.; Filinchuk, Y.; Férey, G. *Science* **2007**, *315*, 1828–1831.

(17) Serre, C.; Millange, F.; Thouvenot, C.; Noguès, M.; Marsolier, G.; Louër, D.; Férey, G. *J. Am. Chem. Soc.* **2002**, *124*, 13519–13526.

(18) Loiseau, T.; Serre, C.; Huguenard, C.; Fink, G.; Taulelle, F.; Henry, M.; Bataille, T.; Férey, G. *Chem.—Eur. J.* **2004**, *10*, 1373–1382.

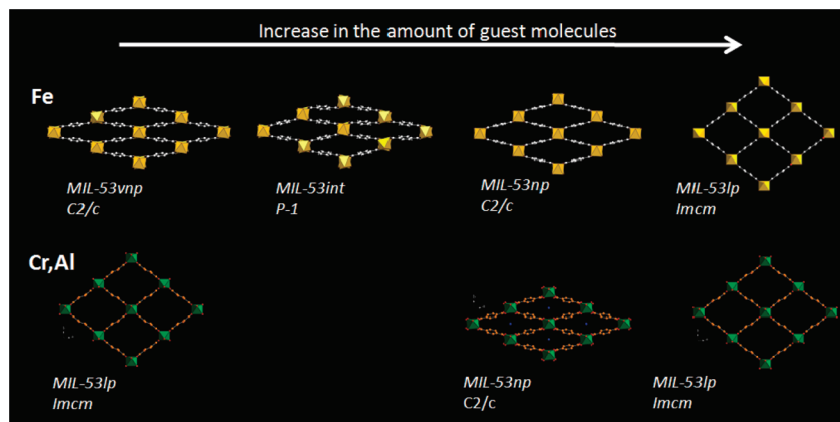


**Figure 1.** Structural evolution of MIL-53(Fe) (top) and MIL-53(Cr,Al) (bottom) with an increase in the amount of guest molecules inside the system (from left to right).

The iron(III) analogue was also described,<sup>21</sup> but in contrast with the Cr and Al based solids, which exhibit a permanent microporosity in the anhydrous state ( $S_{\text{Langmuir}} \approx 1500 \text{ m}^2 \cdot \text{g}^{-1}$ ), its anhydrous form (MIL-53(Fe)-vnp; (vnp for *very narrow pore* form); monoclinic symmetry, space group  $C2/c$  (no. 15),  $V \approx 900 \text{ \AA}^3$ ) exhibits closed pores with no accessible porosity to most gases.<sup>22</sup> Moreover, the breathing behavior of MIL-53(Fe) is more complex than its chromium or aluminum analogues. The transition between the anhydrous (MIL-53(Fe)vnp) and the hydrated forms (MIL-53(Fe)np; space group  $C2/c$ ;  $V \approx 990 \text{ \AA}^3$ ) occurs through the presence of an *intermediate* (MIL-53(Fe)int; space group  $P\bar{1}$  (no. 2);  $V \approx 892 \text{ \AA}^3$ ) triclinic phase where half of the pores are filled with water molecules while the others are closed and empty (see Figure 1).<sup>22,23</sup> The pores nevertheless completely reopen in the presence of organic molecules such as ethanol (MIL-53(Fe)lp; space group  $Imcm$ ;  $V \approx 1560 \text{ \AA}^3$ ),<sup>24</sup> with pore dimensions identical to those observed for the *large pore* form of Al and Cr based MIL-53lp solids. This experimental observation emphasizes that the flexible character of the MIL-53 solids strongly depends on the nature of the metal center, with a different behavior for the Fe analogue compared with the Al and Cr forms.<sup>25</sup> Here, we report the complex adsorption behavior of the MIL-53(Fe) solid in presence of gaseous linear alkanes (C1–C4) at room temperature (303 K). A combination of adsorption isotherms (gravimetric analysis), microcalorimetry, structural analysis (*in situ* synchrotron X-ray Powder Diffraction (XRPD)) and molecular simulation, has been used to establish a correlation between the sorption results and the structural changes related to the flexibility of the MIL-53(Fe) porous solid upon adsorption. For this, a highly leak tight dosing

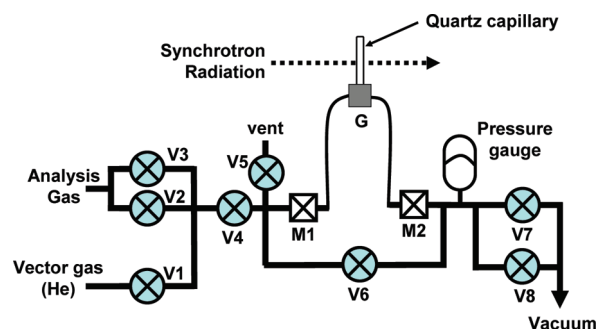


**Figure 2.** Schematic diagram of the dosing manifold.

apparatus has been developed that enables well controlled doses to be introduced to the sample at both low pressures down to  $10^{-2}$  bar and up to 60 bar. This dosing system has been implemented at the Swiss-Norwegian Beamline (SNBL) at the ESRF. It allows the study of the structural behavior of porous solids in the presence of a wide range of gases.<sup>11,19,26</sup> Plausible structural models for the different forms of MIL-53(Fe) present upon the whole adsorption process can be proposed by means of a computational structural determination, starting with the lattice parameters obtained from the refinement of the experimental XRPD pattern. It is then possible using Monte Carlo simulations to explore the geometries of the alkane molecules in the different MIL-53(Fe) forms.

## Experimental Section

**Synthesis.** MIL-53(Fe) was synthesized from a mixture of hexahydrated iron chloride (Alfa, 99%), terephthalic acid (Alfa, 97%), *N,N'*-dimethylformamide (DMF, Alfa, 99%) and fluoroacetic acid (HF, 5M, Prolabo) with a molar ratio of 1:1:280:2 using a Teflon Liner and a metallic Paar Bomb; the mixture was then heated over 12 h to  $150 \text{ }^\circ\text{C}$  and kept at this temperature for 72 h.<sup>22</sup> A yellow powder corresponding to the MIL-53 solid filled with DMF (MIL-53(DMF)) was obtained by filtration. To remove the occluded DMF, the solid was heated at  $150 \text{ }^\circ\text{C}$  on air overnight and then cooled down to room temperature. Further, to extract the residual traces of DMF, the solid was stirred during a few hours in a large volume of deionized water (1 g of MIL-53 in 500 mL of water) and finally filtered and dried at room temperature in air.

- (19) Llewellyn, P. L.; Maurin, G.; Devic, T.; Loera-Serna, S.; Rosenbach, N.; Serre, C.; Bourrelly, S.; Horcajada, P.; Filinchuk, Y.; Férey, G. *J. Am. Chem. Soc.* **2008**, *130* (38), 12808–12814.
- (20) Trung, T. K.; Trens, P.; Tanchoux, N.; Bourrelly, S.; Llewellyn, P. L.; Loera-Serna, S.; Serre, C.; Loiseau, T.; Fajula, F.; Férey, G. *J. Am. Chem. Soc.* **2008**, *130* (50), 16926–16932.
- (21) Whitfield, T. R.; Wang, X.; Liu, L.; Jacobson, A. *J. Solid State Sci.* **2005**, *7*, 1096–1103.
- (22) Millange, F.; Guillou, N.; Walton, R. I.; Grenèche, J.-M.; Margiolaki, I.; Férey, G. *Chem. Commun.* **2008**, 4732–4734.
- (23) Devautour-Vinot, S.; Maurin, G.; Henn, F.; Serre, C.; Devic, T.; Férey, G. *Chem. Comm.* **2009**, *19*, 2733–2735.
- (24) Millange, F.; Serre, C.; Guillou, N.; Férey, G.; Walton, R. I. *Angew. Chem., Int. Ed.* **2008**, *47*, 4100–4105.
- (25) The MIL-53 gallium analogue seems to present an intermediate behavior between the Cr, Al and Fe compounds, see: Volklinger, C.; Loiseau, T.; Guillou, N.; Férey, G.; Elkaim, E.; Vimont, A. *Dalton Trans.* **2009**, 2241–2249.

- (26) Miller, S. R.; Wright, P. A.; Devic, T.; Serre, C.; Férey, G.; Llewellyn, P. L.; Denoyel, R.; Gaberova, L.; Filinchuk, Y. *Langmuir* **2009**, *25* (6), 3618–3626.

**Adsorption Gravimetry/Microcalorimetry.** Adsorption experiments were carried out at 303 K at pressures up to 50 bar using a laboratory made gas dosing system connected to a commercial gravimetric adsorption device (Rubotherm Präzisionsmeßtechnik GmbH).<sup>27,28</sup> A step by step gas introduction mode was used. Prior to each experiment, the sample was outgassed at 250 °C for 16 h. Equilibrium was assumed when the variation of weight remains below 0.03% for 20 min. A typical adsorption experiment takes ca. 24 h. However, due to the flexible character of MIL-53(Fe), much longer equilibrium times as long as 7 days could be obtained for some points.

**Adsorption Coupled with in situ XRPD.** In situ synchrotron X-ray powder diffraction experiments (XRPD) were carried out at the BM01A station at the Swiss Norwegian Beamlines of the European Synchrotron Radiation Facility (Grenoble, France) using a MAR345 imaging plate with a sample-to-detector distance ranging from 150 to 340 mm ( $\lambda = 0.71830$  Å). The data were integrated using the Fit2D program (Dr. A. Hammersley, ESRF) and a calibration measurement of a NIST LaB6 standard sample. The patterns were indexed using the Dicvol software.<sup>29</sup> Le Bail fits were then performed with Fullprof2k software package.<sup>30,31</sup>

The gas dosing system used is schematized in Figure 2. The MIL-53(Fe) sample is introduced inside a quartz capillary of 0.7 mm external diameter which is itself mounted on a T-piece which can be attached to a goniometer head (G). The T-piece is then attached to the system via PEEK capillary (0.8 mm ext. diameter) to a stainless steel manifold via two manual valves (Figure 2). The use of PEEK tubing allows for both pressure resistance to 200 bar and a certain flexibility allowing rotation of the goniometer head when collecting XRPD patterns. In the present system, it is the quartz capillary which determines the upper pressure limit which can be safely used. In the present study, with 0.7 mm capillaries (required to ensure the best contact between solid and gas), a limit of 40 bar was reached. However, a pressure of 60 bars has been attained with the use of 0.5 mm capillaries.

The valve setup itself is mounted on a single rail which is attached to one of the bar mounts around the detector (see photograph in Supporting Information). This allows a minimal manifold encumbrance in the experimental hutch.

The pneumatic valves used (V1–V8, ref Swagelok) along with the rest of the VCR fittings are leak tight and can withstand an overpressure of 250 bar. The manual valves M1 and M2 allow the isolation of the cell if required. The pneumatic valves are operated via an electrovalve block (Joucoumatic) which is connected to an electronic control box (built in house). This controller gives the possibility to action the valves either manually or via a computer.

In a typical experiment, the sample was outgassed separately under a vacuum pressure of  $10^{-3}$  mbar at 250 °C for a few hours. The sample was cooled down to room temperature and transferred under vacuum to the dosing manifold and placed onto the goniometer head. A cryostream was used to adjust the temperature of the sample. The gas was dosed to the manifold and then to the sample. Typical X-ray diffractogram was collected 1 min after the gas introduction, with an acquisition time of 30 s (rotation rate  $1^\circ \text{ s}^{-1}$ ). New X-ray diffraction patterns

were recorded at the same pressure every 5 min, and equilibrium (at a given pressure) was assumed when no change was observed between two successive patterns. When such equilibrium was reached, the pressure was increased and the same procedure applied once again. In the pressure range where a given form (*vnp*, *int*, *np* and *lp*, see below) exists, slight variations of the position of the diffraction peaks are observed, but do not lead to noticeable change of the unit-cells; each form was thus indexed for one pressure only.

**Molecular Simulations.** The initial models for the *narrow pore*, *intermediate* and the *large pore* forms of MIL-53(Fe) were taken from previous studies of water adsorption.<sup>22</sup> For each structural form, the initial cell parameters were thus replaced by those deduced from *in situ* XRPD. All these models were then energy minimized in the space group P1, by keeping the cell parameters fixed, and using the universal force field (UFF) and charges calculated from the Electronegativity Equalization method as implemented in the Materials Studio software.<sup>32</sup> Such strategy based on the same UFF force field has been successfully employed to construct plausible structure of various MILs including the MIL-88 series<sup>33</sup> and more recently the chromium 2,6-Naphtalendicarboxylate MIL-101 system.<sup>34</sup> The convergence criteria were set to  $1.0 \times 10^{-4}$  kcal mol<sup>-1</sup> (energy), 0.005 kcal mol<sup>-1</sup>Å<sup>-1</sup> (forces), and  $5.0 \times 10^{-5}$  Å (displacement) respectively. All of the energy minimizations converged to provide a plausible crystallographic structure for each form of MIL-53(Fe) experimentally detected in presence of the various alkanes. From all of the intermediate, narrow and large pore structures, Monte Carlo simulations using Cerius<sup>2,31</sup> were performed in the NVT ensemble at 303 K to probe the geometries of each C1 to C4 hydrocarbon. A simulation box of 32 rigid unit cells with typically  $3.0 \times 10^6$  MC steps were considered in these calculations. The force fields used to describe the alkane/alkane and alkane/MIL-framework interactions were those previously validated on the MIL-53(Cr)/alkane systems.<sup>19</sup> Short range interactions have been estimated using a cutoff distance of 12 Å and Ewald summation has been used to compute the electrostatic interactions. The partial charges considered for both the hybrid systems and the hydrocarbons as well as the interatomic potential parameters are provided in the Supporting Information.

## Results and Discussion

The study of the alkane adsorption was treated using four different approaches: (i) gravimetric adsorption isotherms at equilibrium (equilibrium criteria at a given pressure: weight variation <0.03% for 20 min.); (ii) *in situ* synchrotron XRPD at equilibrium (equilibrium criteria at a given pressure: two successive identical XRPD patterns collected with an elapsed time of five minutes); (iii) *in situ* synchrotron XRPD out of equilibrium (kinetics of the structural evolution at a given pressure) and (iv) computer simulation using the lattice parameters obtained from the successful indexing of the experimental *in situ* XRPD.

(27) De Weireld, G.; Frere, M.; Jadot, R. *Measurement Sci. Technol.* **1999**, *10* (2), 117–126.

(28) Ghoufi, A.; Gaberova, L.; Rouquerol, J.; Vincent, D.; Llewellyn, P. L.; Maurin, G. *Microporous Mesoporous Mater.* **2009**, *119* (1–3), 117–128.

(29) Boulif, A.; Lotier, D. *J. Appl. Crystallogr.* **1991**, *24*, 987–993.

(30) Rodriguez-Carvajal, J. In *Collected Abstracts of Powder Diffraction Meeting*; Toulouse, France, 1990; pp 127–128.

(31) Roisnel, T.; Rodriguez-Carvajal, J. In *Abstracts of the 7th European Powder Diffraction Conference*; Barcelona, Spain, 2000; Vol. 71.

(32) Accelrys Inc.: San Diego, CA, 2008.

(33) Surlé, S.; Serre, C.; Mellot-Draznieks, C.; Millange, F.; Férey, G. *Chem. Comm.* **2006**, 284–86.

(34) Sonnauer, A.; Hoffmann, F.; Froba, M.; Kienie, L.; Viola, D.; Thommes, M.; Serre, C.; Férey, G.; Stock, N. *Angew. Chem., Int. Ed.* **2009**, *121* (21), 3849–52.

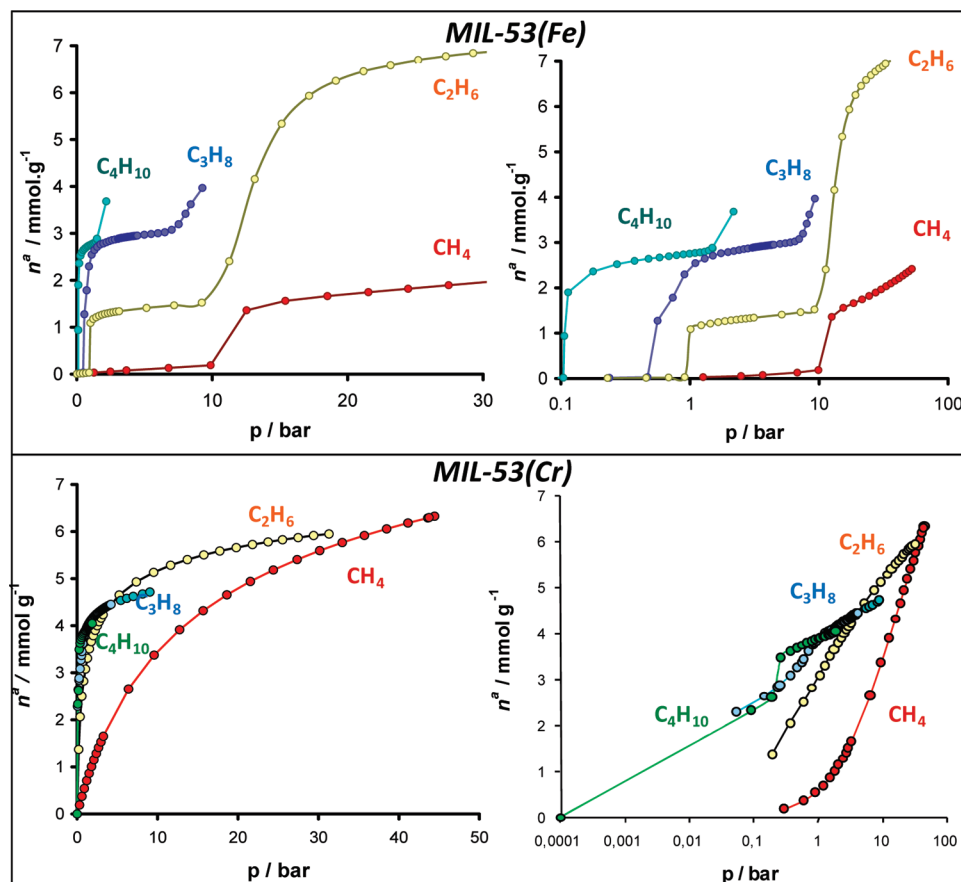


**Figure 3.** Adsorption isotherms of the C1–C4 linear hydrocarbons at 303 K in MIL-53(Fe) (top) and MIL-53(Cr)<sup>19</sup> (bottom): standard coordinates (left); semilog plot (right).

**Adsorption Isotherms at Equilibrium.** Adsorption isotherms at 303 K are shown in Figure 3, both in standard and in semilog forms in order to highlight the low pressure steps. Indeed, for all the hydrocarbon molecules, steps in the isotherms can be clearly distinguished. The smaller molecule, methane, shows a negligible uptake up to 10 bar, followed by a step which leads to an adsorbed amount of around 1.4 mmol·g<sup>-1</sup> at higher pressure. The adsorption of the other investigated linear hydrocarbons (ethane, propane, butane) leads to a first step in the isotherm occurring for a similar amount of adsorbed species even if it is not so apparent for butane. However, this step was confirmed in the XRPD experiments. A second step is also detected for propane and an inflection may be observed in the butane isotherm which both correspond to an uptake of about 2.8 mmol g<sup>-1</sup>. Finally a further step is also observable for the C2–C4 hydrocarbons although not always complete in these isotherms. For ethane, after a step at low pressure obtained for an adsorbed amount around 1.2 mmol g<sup>-1</sup>, a larger step at higher pressure of 6.6 mmol g<sup>-1</sup> is assigned to a complete filling of the pores. The *in situ* XRPD investigations shown below indicate that each step corresponds to a different degree of pore opening of the MIL-53(Fe).

Further, the pressure of the uptake steps decreases as the length of the hydrocarbon chain increases. This behavior can be related to the increase of the van der Waals interactions between the alkane and the MIL-framework. The number of steps observed strongly depends on the pressure range selected to run the adsorption experiments. Indeed, for C1, other steps would probably occur at higher pressures using the same temperature of 303 K. In addition, for the longer alkanes

(propane and butane), it was not possible to apply pressures higher than the saturation vapor pressure of 1.8 and 10 bar, respectively, at 303 K. Nevertheless, one cannot rule out that other adsorption steps in the isotherms could be obtained for MIL-53(Fe) at lower temperatures.

The gas adsorption behavior of MIL-53(Fe) is very different from that previously observed for the Cr or Al MIL-53 analogues (see Figure 3) in which gas uptake occurs even at low pressure, despite some breathing effects occurring for longer (C2–C4) linear alkanes.<sup>19,20</sup> This observation thus emphasizes a different breathing ability depending on the nature of the metal center (see above).

**In situ XRPD at equilibrium.** In situ XRPD patterns collected on MIL-53(Fe) during the adsorption of the linear alkanes (C1–C4) (Figure 4) show unambiguous changes in the crystal-line structure as a function of the gas adsorption into the channels. Except for methane, where only one structural change is observed in a wide range of pressure up to 40 bar, three structural transformations are present for the longer alkanes (ethane, propane, butane), with different XRPD signatures according to the gas pressure. Moreover, the pressures associated with these structural changes are on the whole in very good agreement with the ones corresponding to the steps observed in the adsorption isotherms. These small differences may be related to the difference in equilibrium criteria used for each study, the one chosen for the isotherms measurements being the most severe. The comparison between both results nevertheless clearly proves that the steps are associated with structural modifications.

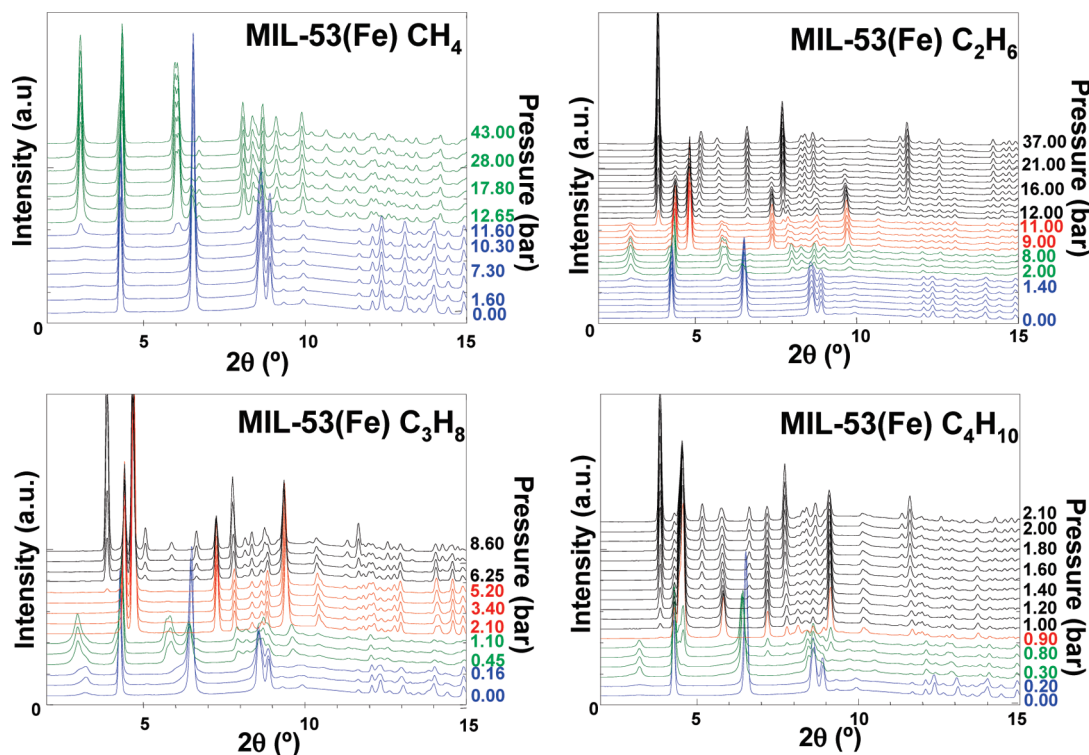


**Figure 4.** Adsorption of linear alkanes on MIL-53(Fe) at 303 K followed by XRPD. The color corresponds to the major phase observed at the given pressure: blue, anhydrous *very narrow pore* form; green, *intermediate* form; red, *narrow pore* form; black, *large pore* form.

**Table 1.** Cell Parameters of MIL-53(Fe) *Intermediate* Form in Presence of C1–C4 Hydrocarbons (Space Group  $P\bar{1}$  or  $P1$ )

gas	<i>a</i> (Å)	<i>b</i> (Å)	<i>c</i> (Å)	$\alpha$ (deg)	$\beta$ (deg)	$\gamma$ (deg)	<i>V</i> (Å <sup>3</sup> )	<i>P</i> (bar)	<i>n</i> ads (from gravimetry) mmol g <sup>-1</sup>
CH <sub>4</sub>	15.138(1)	10.631(1)	6.888(1)	104.634(6)	108.086(5)	102.793(5)	963.8(1)	43	2.1 < <i>n</i> < 2.27
C <sub>2</sub> H <sub>6</sub>	14.440(3)	10.370(2)	6.989(1)	98.27(2)	92.18(2)	107.54(1)	983.8(3)	4.0	1.34 < <i>n</i> < 1.41
C <sub>3</sub> H <sub>8</sub>	14.662(2)	10.380(3)	6.944(1)	98.66(2)	93.43(2)	105.56(1)	1001.0(2)	1.1	<i>n</i> ≈ 1.3
C <sub>4</sub> H <sub>10</sub>	14.651(3)	10.514(3)	6.998(1)	99.24(2)	91.98(2)	106.95(1)	1014.0(2)	1.6	<i>n</i> ≈ 1

**Table 2.** Cell Parameters of MIL-53(Fe) *Narrow Pore* Form in Presence of C1–C4 Hydrocarbons (Space Group  $C2/c$  or  $Cc$ )

gas	<i>a</i> (Å)	<i>b</i> (Å)	<i>c</i> (Å)	$\beta$ (deg)	<i>V</i> (Å <sup>3</sup> )	<i>P</i> (bar)	<i>n</i> ads (from gravimetry) mmol g <sup>-1</sup>
C <sub>2</sub> H <sub>6</sub>	19.340(4)	9.405(2)	6.834(1)	107.44(2)	1185.8(4)	12.0	2.40 < <i>n</i> < 4.16
C <sub>3</sub> H <sub>8</sub>	19.570(1)	9.966(1)	6.870(1)	108.34(1)	1272.0(3)	4.8	2.95 < <i>n</i> < 2.97
C <sub>4</sub> H <sub>10</sub>	19.991(1)	10.3037(8)	6.8885(4)	112.513(3)	1310.7(1)	1.6	2.87 < <i>n</i> < 3.68

**Table 3.** Cell Parameters of MIL-53(Fe) *Large Pore* Form in Presence of C1–C4 Hydrocarbons (Space Group  $I m c m$ )

Gas	<i>a</i> (Å)	<i>b</i> (Å)	<i>c</i> (Å)	<i>V</i> (Å <sup>3</sup> )	<i>P</i> (bar)	<i>n</i> ads (from gravimetry) mmol g <sup>-1</sup>
C <sub>2</sub> H <sub>6</sub>	15.871(1)	14.483(1)	6.9037(2)	1586.9(1)	37.0	7.00 < <i>n</i>
C <sub>3</sub> H <sub>8</sub>	16.232(1)	13.980(2)	6.897(1)	1565.0(3)	7.6	3.19 < <i>n</i> < 3.42
C <sub>4</sub> H <sub>10</sub>	16.013(1)	14.187(1)	6.8917(4)	1565.7(2)	2.1	2.87 < <i>n</i> < 3.68

The starting outgassed MIL-53(Fe) solid (blue in Figure 4) corresponds to the anhydrous phase (MIL-53(Fe)-vnp) (monoclinic symmetry, space group  $C2/c$  ( $n^\circ 15$ ),  $V=904(1)$  Å<sup>3</sup>, i.e. with closed pores,<sup>22</sup> and no accessible free volume to accommodate guest molecules. Upon an increase of the gas pressure, a new characteristic diffraction pattern appears (labeled *intermediate*, green in Figure 1), which can be satisfactorily indexed for all alkanes in a triclinic setting, space group  $P\bar{1}$  with a unit cell varying from 963.8(1) to 1014.0(1) Å<sup>3</sup> depending on the size of the probe molecule (Tables 1, 2, and 3). This *intermediate* structure was already observed during the dehydration of MIL-53(Fe) and corresponds to a partial opening of one every second pore.<sup>22,23</sup> One can also notice that this *intermediate* form only exists in a narrow range of pressure for the heavier alkanes

(C2–C4) (see Figure 4) and is always observed in mixture with the other forms (either MIL-53(Fe)-np or MIL-53(Fe)-vnp, see Figure 4), indicating probably the coexistence of crystallites of different pore sizes with various alkane loadings for a given pressure. Indeed, at higher pressure, except for methane, a *narrow pore* form (red in Figure 4) is observed, which is indexed in the monoclinic space group  $C2/c$ , with a unit cell volume ranging from 1185.8(1) to 1310.7(1) Å<sup>3</sup> depending on the guest molecule (Table 2). This unit cell is similar to the one observed

(35) Rosenbach, N.; Jobic, H.; Ghoufi, A.; Salles, F.; Maurin, G.; Bourrelly, S.; Llewellyn, P. L.; Devic, T.; Serre, C.; Férey, G. *Angew. Chem., Int. Ed.* **2008**, *47*, 6611–6615.

(36) Salles, F.; Jobic, H.; Maurin, G.; Koza, M. M.; Llewellyn, P. L.; Devic, T.; Serre, C.; Férey, G. *Phys. Rev. Lett.* **2008**, *100* (24), 245901–4.

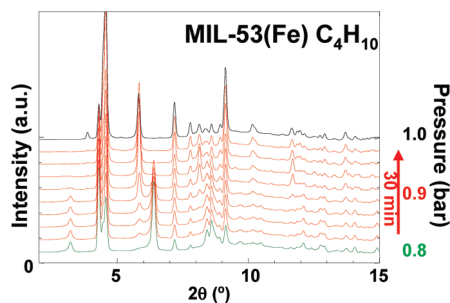


**Figure 5.** Kinetic evolution of the XRPD pattern of MIL-53(Fe) at 0.9 bar of butane at 303 K. The colors correspond to the major phase observed at the given pressure: green, *intermediate*; red, *narrow pore*; black, *large pore* form.

for MIL-53(M) (M = Cr, Al)<sup>7,18</sup> with intermediate loading of CO<sub>2</sub>, H<sub>2</sub>O and linear alkanes (C1–C4), and corresponds to the partial opening of all the pores. Compared to the *intermediate* form, its sorption capacity should be nearly double, which is clearly visible in the adsorption isotherm for propane. Finally, at higher pressures, a new pattern is observed (black in Figure 2), which is indexed in the orthorhombic Imcm space group, and corresponds to the *large pore* form (unit cell volume ranging from 1565.9(1) to 1586.7(1) Å<sup>3</sup>), as already observed upon the adsorption of some liquids in MIL-53(Fe),<sup>24</sup> and of various gaseous species in MIL-53(Cr).<sup>11,19</sup>

**In-situ XRPD Out of Equilibrium.** Although the diffusivity of small apolar species in other MIL-53 solids has been proved to be rather fast,<sup>35,36</sup> we already noticed that the diffusion of the longer linear alkanes, when associated with flexibility, could be slow.<sup>20</sup> In the case of MIL-53(Fe), the measurement of the complete adsorption isotherm took up to 5 and 7 days for propane and butane, compared to 14 h for methane and ethane. The equilibrium times could reach 24 h at low pressure for a single point when the phase transformation is occurring (from 0.56 to 0.9 bar for butane). As the pores are initially closed, adsorbates have to “force” their entrance into the solid, which could explain such long equilibration times. In order to isolate the XRPD pattern of the *intermediate* and *narrow pore* form

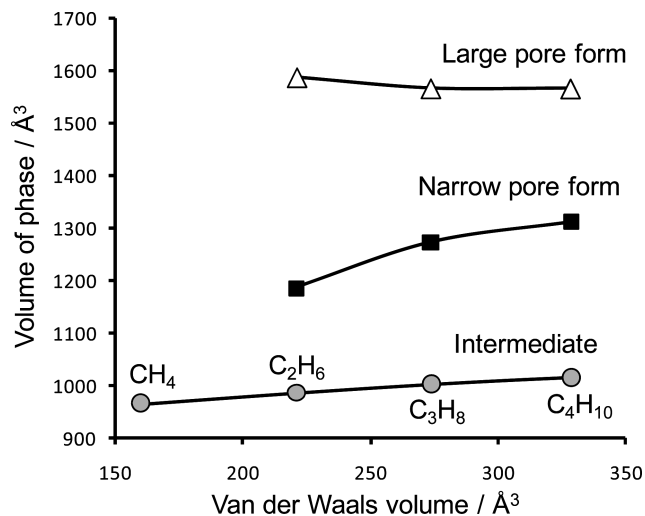


**Figure 7.** Unit cell volume of the various MIL-53(Fe) phases at 303 K as a function of the van der Waals volumes of the probe molecules.

for butane adsorption in a reasonable amount of time, a pressure above the adsorption step (from the isotherm) was applied, and several XRPD patterns were collected at this pressure for 30 min. The kinetic evolution from the *intermediate* to the *large pore* form through the *narrow pore* form leads to changes in the relative proportions of each phase as typically illustrated in Figure 5 for butane. Although the equilibrium time for the phase transformation at low pressures for the long chain alkanes is rather high, this experiment, performed out of equilibrium, allowed us to isolate the XRPD diagram of each form, and then to deduce the experimental cell parameters used for simulation.

**Computer Simulation.** The computational strategy described above was then employed to determine the structures of each MIL-53(Fe) form in the presence of the different alkanes, starting with the lattice parameters obtained from indexing of the experimental powder XRPD. This approach allowed us to avoid the time-consuming process of an *ab initio* structure determination from the powder data for each MIL-53(Fe) form/hydrocarbon pair. All of these predicted structures are provided

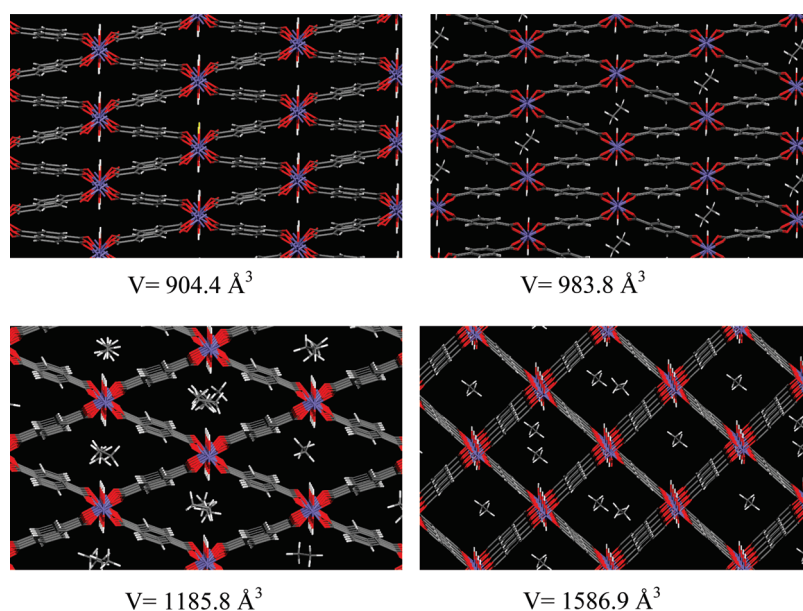


**Figure 6.** Illustration of the structural behavior of the MIL-53(Fe) solid upon ethane adsorption (simulated structures): *very narrow pore* (top left), *intermediate* (top right), *narrow pore* (bottom left), and *large pore* (bottom right) forms. Cell volumes are also indicated.

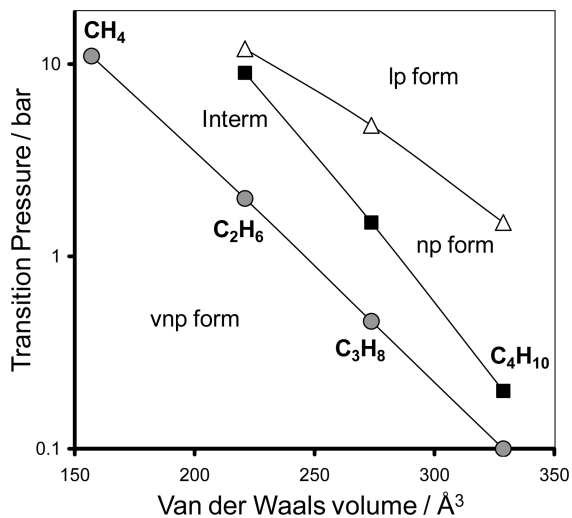


**Figure 8.** Variation of the transition pressures of MIL-53(Fe) at 303 K as a function of the van der Waals volumes of the alkane molecules.

in the Supporting Information. A further step consisted of probing the geometries of C1–C4 in these different MIL-53(Fe) versions as previously described. We observed whatever the considered MIL-53(Fe) forms, that the hydrocarbons are mainly interacting with both the hydroxyl groups and the phenyl rings of the MIL-surface with characteristic distances separating the hydrogen of the alkane molecule and both the organic and inorganic parts of the framework ranged from 3.2 to 3.8 Å. Further, the simulated C<sub>2</sub>–C<sub>4</sub> adsorption geometries show that the number of interaction sites between the hydrocarbon molecules and the MIL framework increases with the chain length of the alkane molecule. These arrangements are similar to those previously observed in the narrow and large pore forms of the MIL-53(Cr) system.

As a typical illustration, we report in Figure 6 the various structural forms of MIL-53(Fe) observed during the adsorption of ethane where one can easily observe the progressive stepwise opening of the structure from the *very narrow* to the *large pore* forms.

A phenomenological analysis of the whole experimental observations consisted of relating the cell volume of the MIL-53(Fe) phase (for a given form) and the van der Waals volume of the adsorbed probe molecule. Figure 7 shows the unit cell volumes of the *intermediate*, *narrow pore* and *large pore* form of MIL-53(Fe) as a function of the van der Waals volume of the probe molecule. It can be seen for the considered hydrocarbons that the volume of both intermediate phases slightly increases with increasing volume of the probe molecule. Although the flexibility of the hydrocarbons is not considered, this approach suggests that the pore opening of the *intermediate* and *narrow pore* phases is adjusted to accommodate the probes, increasing the unit cell volume of the phases as the probes increase in volume. This is also consistent with the fact that, although the sorption behavior of MIL-53(Cr) and (Fe) are

different, the cell parameters of their *narrow pore* forms are very similar.<sup>19</sup> Interestingly, the unit cell volume of the large pore form, observed with this series, is more or less the same whatever the volume of the probe molecule. This trend can be explained by the fact that this corresponds to a total filling of the pores even if under these experimental conditions, the maximum of adsorption has not been reached but this is compensated in terms of loading by the presence of various amounts of the *narrow pore* form.

In addition, one can also notice that the pressure, at which the different structural transitions occur, identified from the XRPD patterns and/or the isotherms decrease as the size of the hydrocarbon increases (Figure 8).

## Conclusions

This study reports the adsorption of short alkyl chain alkanes in the flexible porous metal-organic framework MIL-53(Fe) by combining gravimetry measurements and *in situ* Synchrotron XRPD using a specifically designed adsorption apparatus. From the *in situ* XRPD analysis, molecular simulations were performed to define the various structural forms of MIL-53(Fe) present upon the whole adsorption process. Comparing with the chromium or aluminum MIL-53 analogues, the iron MIL-53 solid exhibits a more complex behavior with a multistep pore opening process occurring at pressures which shows that the breathing behavior strongly depends on the nature of the alkane. This difference is (at least) related to the fact that the Al and Cr solids exhibit open pores in its anhydrous state (*lp* form), whereas the Fe based solid presents only closed pores (*vnp* form). Nevertheless, even if the adsorption isotherms are different, similar intermediate states (*np* form) are observed. The appearance of such partial pore opening in the flexible MIL-53 solids is thus related to host–guest interactions and adequate fits between the pore size and its content rather than to the chemical nature of the framework. Although the adsorption of mixtures of gases has not been studied yet, the different affinity of the MIL-53(Fe) framework for the hydrocarbons, according to the length chain, might lead to applications in separation.

**Acknowledgment.** We are grateful for financial supports provided by french ANR-SAFHS (ANR-07-BLAN-0284-02), NOMAC (ANR-06-CO2-008) and EU INSIDE PoRES (NMP3-CT-2004-500895) as well to the ESRF for providing access to the Swiss-Norwegian beamline. F. Millange is acknowledged for providing samples of MIL-53(Fe).

**Supporting Information Available:** Various images of the experimental setup at the ESRF, Tables, and description of the partial charges for both alkanes and MIL-53(Fe) as well as the interatomic potentials used for the molecular simulation. CIF images obtained from the molecular simulation study are also available. This material is available free of charge via the Internet at <http://pubs.acs.org>.

JA902740R